Equilibrium energy spread and emittance in a Compton ring:
An alternative approach

I. Chaikovska[*] and A. Variola[†]

Laboratoire de l'Accélérateur Linéaire (LAL), Université Paris-Sud XI,
CNRS/IN2P3, 91898 Orsay, France

In this article the Campbell's theorem is used to evaluate the equilibrium emittance and energy spread in a Compton ring. This method allows us to have an efficient analytical approach separating the contributions of the Compton cross section from the luminosity factor. The consequent advantage is given by the possibility to have an easy extrapolation for the "nonclassical" cases like the polarized Compton backscattering or the evaluation of the equilibrium given by different radiation mechanisms. The effects accounting for the polarized Compton backscattering in the article are evaluated numerically. The analytical results in the nonpolarized case and in the negligible recoil effect approximation are in excellent agreement with the values obtained by matching the Compton damping rate with the quantum fluctuations, and they show that the equilibrium energy spread and emittance are independent from the luminosity.

I. INTRODUCTION

A. Interest of Compton sources

At present there is a growing interest in radiation sources based on the Compton backscattering effect [1]. This is the consequence of the very important energy boost acquired by the backscattered photon which allows us to provide hard X-/gamma ray sources with relatively moderate accelerator beam energies. In the past, these sources have not been largely exploited due to the low emitted flux given by the Compton/Thomson cross section. Nowadays, the impressive technology advances in high (average and peak) power lasers, in the stabilization of high gain optical amplifiers [2], in the optical recirculator design [3], and in the accelerator technology give the opportunity to envisage compact Compton backscattering sources (CBS) with possible applications in different applied fields. Moreover, the energy-angle kinematic dependence of the emitted photons makes
it possible to obtain a quasimonochromatic X-/gamma ray beam (monochromaticity of the order of a percent) using a simple diaphragm system. Different user communities are therefore studying the possible applications of CBS in, for example, the field of protein crystallography, medical science, and cultural heritage [4,5]. Nuclear science applications are also taken into account with the production of

gamma rays for fundamental physics research [6] and nuclide detection [7,8].

A wide spectrum of applied science communities will profit from all these experimental programs with different requirements on the emitted photon beam characteristics determining the accelerator-laser system design. Linear accelerators coupled with high peak lasers are usually envisaged for the high brilliance applications. On the other side, a high average flux need is covered either by the superconductive linacs [also in the Energy Recovery configuration (ERL)] [9,10] or by the Compton rings [11,12] associated with high average power lasers amplified in passive optical resonators [13].

B. Circular Compton sources

As far as the Compton rings are concerned different projects are being developed. Pioneering experimental activities in the field of gamma ray production have been worked out in ADONE [14], Novorsibirsk [15], Super ACO [16], Duke University [17], and ESRF [18]. In the TERAS ring 2×10^4 gamma rays per second in the MeV energy range were produced by Compton scattering [19]. In SPring-8 the achieved flux reached 2.5×10^6 gamma rays per second at 2.4 GeV photon energy. Experiments of the FEL intracavity photon-electron scattering in the UVSOR ring [20] also provided a flux of 2×10^6 gamma rays per second using a 20 W laser power. Duke University developed a strong research program in its storage ring [21]. This allows us to reach a stored laser power in the kW regime increasing the emitted flux up to a few 10^{10} gamma rays per second with a photon energy cutoff of 100 MeV. In the X-ray domain the only operating storage ring is the one constructed by Lyncean Technologies Inc. [22]. It produces an average flux of 10^{11} X-rays per second in the

---

[*]chaikovs@lal.in2p3.fr
[†]variola@lal.in2p3.fr

10–20 keV energy range by means of an optical system based on a high gain Fabry-Perot resonator. Other projects, always based on the high gain optical resonators, are ThomX [4] and NESTOR [23] at present in the construction phase. Here, the increased electron beam energy and optical resonator gain should allow to reach the 10^{12}–10^{13} X-rays per second flux regime emitting photons up to 89 keV for ThomX and 900 keV for NESTOR.

II. CIRCULAR COMPTON SOURCES

A. Beam dynamics

In the past, Compton backscattering of laser photons off the high energy electrons has been proposed in the Linear Collider framework [24] as a method to cool a multi-GeV electron beam through radiation damping. Then, in [25], the authors proposed a compact laser-electron storage ring in the tens of MeV energy range for electron beam cooling and X-ray generation. At higher energy (few GeV) CBS can be employed for gamma ray generation [26] aiming at the nuclear applications and positron production.

For all the different applications requiring different beam energies different regimes have to be taken into account as far as the CBS beam dynamics is concerned because of the energy quadratic dependence of the backscattered photon energy and consequently of the electron recoil. At low energy, due to the short beam lifetime and low synchrotron power emitted, the Compton contribution defines the equilibrium emittance and energy spread. At higher energy the strong electron recoil at the Compton cutoff also has to be taken into account since it can drive the electron outside the rf bucket, increasing the beam losses. So, the Compton scattering can be treated as a "quantum noise" to be added to the synchrotron cooling and quantum fluctuation contributions. Moreover, for the applications involving polarized beams, it is also important to estimate the equilibrium properties accounting for the polarization of the initial states. The dynamics of the electron beam under the Compton scattering regime is thus considered a critical point of a Compton ring design as a function of the beam energy and the emitted flux.

B. Compton backscattering kinematics and cross section

Compton backscattering describes the process $\gamma\, e^- \to \gamma e^-$, where the scattered photon acquires part of the electron kinetic energy. The kinematics imposes that the electron undergoes a recoil after the emission as described on Fig. 1, where E_e, E_γ, and E_L are, respectively, the incident electron, the scattered photon, and the laser photon energies; ϕ and θ_e are the collision and the scattered electron recoil angles.

The Compton backscattering effect can be also seen like the emission of radiation by the electrons oscillating in the laser field [27], as in an undulator. The angular distribution
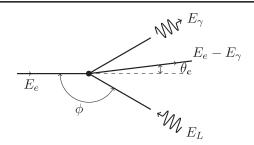

FIG. 1. The kinematics of the Compton scattering.

of the scattered photons is thus concentrated within the typical $\sim 1/\gamma$ opening angle cone around the direction of motion of the electrons.

The product of the total Compton cross section times the luminosity determines the emitted flux. The differential cross section gives the spectral content. To define the Compton scattering cross section, it is convenient to define two dimensionless variables [28]:

$$x = 2\gamma \frac{E_L}{m_e c^2}(1 - \beta \cos\phi) \quad \text{and} \quad y = \frac{E_\gamma}{E_e} \leq y_m = \frac{x}{x+1},$$

(1)

where $\beta = \frac{v}{c}$ and $\gamma = \frac{1}{\sqrt{1-\beta^2}}$ is the Lorentz factor. For the Compton scattering of the laser light when $\gamma E_L \ll m_e c^2$, one usually has $x \ll 1$. If "head-on" collisions ($\phi = \pi$, $x = 4\gamma^2 E_L/E_e$) are taken into account, the E_γ maximum value (energy spectrum cutoff) is $E_\gamma^{\max} \approx 4\gamma^2 E_L$.

Considering the most general case of a polarized laser colliding with a polarized electron beam, the photon energy spectrum is given by the differential cross section summed over the spin states of the final particles [28,29]:

$$\frac{d\sigma_c}{dy} = \frac{2\pi r_e^2}{x}\left(\frac{1}{1-y} + 1 - y - 4r(1-r)\right.$$
$$\left. + P_e P_c r x (1-2r)(2-y)\right),$$

(2)

where $r_e = \frac{e^2}{m_e c^2} \approx 2.82 \times 10^{-15}$ m is the classical electron radius, P_e is twice the helicity of the initial electron, P_c stands for the laser photon degree of the circular polarization (initial photon helicity), and

$$r = \frac{y}{x(1-y)} \leq 1.$$

(3)

The total Compton cross section can be written then as a sum of two terms [29]:

$$\sigma_c = \sigma_c^{np} + P_e P_c \sigma_0,$$

(4)

where σ_c^{np} is the Compton cross section for unpolarized particles given by

$$\sigma_c^{np} = 2\pi r_e^2 \frac{1}{x} \left[\left(1 - \frac{4}{x} - \frac{8}{x^2} \right) \ln(1+x) + \frac{1}{2} + \frac{8}{x} \right.$$
$$\left. - \frac{1}{2(1+x)^2} \right], \qquad (5)$$

and σ_0 reads

$$\sigma_0 = \frac{2\pi r_e^2}{x} \left(\left(1 + \frac{2}{x} \right) \ln(1+x) - \frac{5}{2} + \frac{1}{x+1} - \frac{1}{2(1+x)^2} \right). \qquad (6)$$

It is important to point out, that for circularly polarized laser photons, the differential and the total Compton cross sections [see Eqs. (2) and (4)] do not depend on the transverse polarization of the initial electrons. This is correlated to the storage rings case where the particle spin precesses around the dipole magnetic field, so it is transversal in respect to the longitudinal momentum. Moreover, for the linear polarized laser photons the cross sections do not depend at all on the polarization of the initial electrons [30]. The total Compton cross section for the polarized initial states [see Eq. (4)] differs from the unpolarized case only if the laser photon is circularly polarized and the electron has nonzero projection of the spin onto the direction of momentum.

In the case when $x \ll 1$, the unpolarized total Compton cross section given by Eq. (5) as a function of x can be expanded into Taylor series and so

$$\sigma_c^{np} \approx 2\pi r_e^2 \frac{4}{3}(1-x) \approx \sigma_T(1-x) \qquad (7)$$

the total Compton cross section is nearly equal to the classical Thomson cross section $\sigma_T = 8\pi r_e^2/3 \approx 6.65 \times 10^{-29}$ m^2.

III. ELECTRON BEAM ENERGY SPREAD AND EMITTANCE CALCULATIONS BY CAMPBELL'S THEOREM

A. Campbell's theorem

As previously said, Compton backscattering in the CBS may be considered as a shot noise process and therefore treated by taking into account Campbell's theorem evaluating the average effect of Poisson excitation processes on different distributions [31].

In general, the shot noise function $s(t)$ can be seen as random fluctuations in the output of a linear system activated by a series of Poisson δ-events $x_0(t)$, e.g., photon emission or electron-photon scattering, occurring at the random time t_i:

$$s(t) = \sum_i a g(t - t_i) \quad \text{with} \quad x_0(t) = \sum_i a\delta(t - t_i), \quad (8)$$

where a is the amplitude of the δ-excitation and $g(t)$ is the response of the system. In this framework, Campbell's theorem [32–34] provides the information about the first and second central momenta of the probability distribution describing such a process.

Assuming a linear dynamic system and knowing its response to a δ-excitation occurring randomly in time with average frequency f, the second central momentum or variance of the process σ_s^2 is

$$\sigma_s^2 = a^2 f \int_{-\infty}^{+\infty} g^2(t - t_0) dt. \qquad (9)$$

If a series of excitations occurs randomly in time, with amplitude distribution $\dot{n}(a)$, Eq. (9) can be written in a more general form as:

$$\sigma_s^2 = \int_0^\infty a^2 \dot{n}(a) da \int_{-\infty}^{+\infty} g^2(t - t_0) dt = \mathcal{A}\mathcal{G}, \qquad (10)$$

where $\mathcal{A}$ is the integral describing the second order moment of the excitation distribution and $\mathcal{G}$ is the integral over the response function.

It seems therefore possible to apply Campbell's theorem to obtain the equilibrium energy spread and transverse emittance in a Compton ring taking into account the photon-electron scatterings as the statistical events affecting the particle dynamical state and the betatron and energy oscillation damping as the system response.

B. Equilibrium energy spread and emittance induced by Compton scattering

In absence of Compton scattering the beam dynamics provide a Gaussian equilibrium longitudinal and transverse distributions [35]. As far as the longitudinal phase space is concerned, as previously mentioned, the electron beam energy spectrum is modified by the laser photon-electron interaction quantum excitation. The equilibrium energy spread, defined through the square root of the variance of the electron energy distribution $\sqrt{\sigma_{\text{Comp}}^2}$, can be derived on the basis of Campbell's theorem.

In the transverse phase space a photon emission with angle θ_γ gives to the electron a recoil resulting in a transverse deflection θ_e and consequently in the transverse emittance variation. Assuming that the Compton interaction region corresponds to a beam waist (that is straightforward if the luminosity has to be maximized), it is given that $\epsilon = 2\langle\theta_e^2\rangle\beta^*$, where β^* is the electron betatron function in the interaction point (IP) [36]. The equilibrium transverse emittance ϵ can also be evaluated by means of the variance of the electron transverse angular deflection $\langle\theta_e^2\rangle$.

In a storage ring the response of the electron to a δ-pulse excitation (Compton scattering) at the time $t_0 = 0$ can be seen as the damped betatron and synchrotron oscillations

[36,37]. Projecting on the transverse and longitudinal planes these oscillations read respectively:

$$g_B(t) = \theta_e e^{-\alpha_B t} \cos(\Omega_b t), \qquad (11)$$

$$g_S(t) = E_\gamma e^{-\alpha_E t} \cos(\Omega_s t), \qquad (12)$$

where $g_0 = E_\gamma$ or θ_e is the initial electron energy variation or transverse deviation; α_B, α_E and Ω_b, Ω_s are, respectively, the damping rates and frequencies of the transverse (betatron) and longitudinal (synchrotron) modes of electron oscillations.

According to Eq. (10), we can now calculate the integral $\mathcal{G}$ for the two different modes of oscillations. In general form it can be written as

$$\mathcal{G} = \frac{1}{g_0^2} \int_{t_0}^{\infty} g^2(t-t_0)dt = \frac{1}{g_0^2} \int_0^{\infty} g^2(t)dt$$
$$= \int_0^{\infty} (e^{-\alpha t} \cos\Omega t)^2 dt = \frac{\alpha}{4(\Omega^2 + \alpha^2)} + \frac{1}{4\alpha}. \qquad (13)$$

Usually, the damping rate in the storage rings, of the order of tens of Hz, is relatively small in respect to the synchrotron and betatron frequencies, so $\alpha \ll \Omega$ and it is possible to neglect the first term in Eq. (13) resulting in

$$\mathcal{G} = \frac{1}{4\alpha}. \qquad (14)$$

The damping rate α can be expressed in the following way for all three degrees of freedom:

$$\alpha_i = J_i \alpha_0 = J_i \frac{\langle P_\gamma \rangle}{2E_e} \qquad (15)$$

with

$$J_x = 1 - \mathcal{D}, \quad J_y = 1, \quad J_e = 2 + \mathcal{D}, \quad \sum_i J_i = 4, \qquad (16)$$

where $\langle P_\gamma \rangle$ is the average rate of the electron energy loss, E_e is the electron beam energy, J_i are the damping partition numbers, and $\mathcal{D}$ is a quantity (number) which depends on the property of the guide field [35,38]. So, the inverse of the damping rate can be seen as the time it takes for the electron to radiate its energy. To a large extent, considering a ring with a design orbit lying in the horizontal plane and a magnetic field which is homogeneous and symmetric in respect to that plane, $\mathcal{D}$ is a fairly small number [35]. In this case, the damping rate of synchrotron oscillations is twice the transverse damping rate.

Now, taking into account that the total flux of scattered photons can be evaluated as a product of the luminosity by the Compton cross section, the damping rates can be formulated as:

$$\alpha_E = \frac{\langle E_\gamma \rangle \mathcal{F}}{E_e} = \frac{\langle E_\gamma \rangle \mathcal{L} \sigma_c}{E_e} \quad \text{and}$$

$$\alpha_B = \frac{\langle E_\gamma \rangle \mathcal{F}}{2E_e} = \frac{\langle E_\gamma \rangle \mathcal{L} \sigma_c}{2E_e}, \qquad (17)$$

where $\mathcal{F}$ is the flux of the scattered photons, $\mathcal{L}$ is the luminosity of the Compton collisions, σ_c is the total Compton scattering cross section, and E_γ is the energy of the emitted photon for which the average is

$$\langle E_\gamma \rangle = \frac{\int_{E_L}^{E_\gamma^{\max}} E_\gamma \frac{d\sigma_c}{dE_\gamma} dE_\gamma}{\int_{E_L}^{E_\gamma^{\max}} \frac{d\sigma_c}{dE_\gamma} dE_\gamma}. \qquad (18)$$

The integration in Eq. (18) goes in the interval from the energy of the laser photons E_L up to the Compton energy cutoff $E_\gamma^{\max}$.

Therefore, in order to evaluate the variance of the energy and angular spreads, one has to plug the damping rates [see Eq. (17)] into Eq. (13) separately for the two modes of oscillations and then insert it into Eq. (10) knowing that for the synchrotron oscillations:

$$\mathcal{A}_\mathcal{E} = \int_0^{\infty} a^2 \dot{n}(a) da = \int_{E_L}^{E_\gamma^{\max}} E_\gamma^2 \dot{n}(E_\gamma) dE_\gamma$$
$$= \int_{E_L}^{E_\gamma^{\max}} E_\gamma^2 \mathcal{L} \frac{d\sigma_c}{dE_\gamma} dE_\gamma, \qquad (19)$$

whereas for the betatron ones:

$$\mathcal{A}_\mathcal{B} = \int_0^{\infty} a^2 \dot{n}(a) da = \int_0^{\theta_e^{\max}} \theta_e^2 \dot{n}(\theta_e) d\theta_e$$
$$= \int_0^{\theta_e^{\max}} \theta_e^2 \mathcal{L} \frac{d\sigma_c}{d\theta_e} d\theta_e, \qquad (20)$$

where $\dot{n}(E_\gamma)$ and $\dot{n}(\theta_e)$ are the fluxes expressed, respectively, in energy and angular coordinates, given by the product of the luminosity times the spectral density of the photons. It still will be convenient to change the variable of integration in Eq. (20) to E_γ. Given $d\sigma_c/d\theta_e = (d\sigma_c/dE_\gamma)(dE_\gamma/d\theta_e)$, $\mathcal{A}_\mathcal{B}$ can be written as:

$$\mathcal{A}_\mathcal{B} = \int_0^{E_\gamma(\theta_e^{\max})} \theta_e^2(E_\gamma) \mathcal{L} \frac{d\sigma_c}{dE_\gamma} dE_\gamma. \qquad (21)$$

where $E_\gamma(\theta_e^{\max})$ is the scattered photon energy corresponding to the maximum value of the scattered electron angle $\theta_e^{\max}$ in the given interval and can be evaluated taking into account the well-defined relationship between the energy and the scattering angle in the Compton scattering [39]:

$$\theta_e^2(E_\gamma) = \frac{E_\gamma^{\max}E_\gamma - E_\gamma^2}{E_e^2\gamma^2}. \tag{22}$$

Finally, taking into account Eqs. (10), (14), and (17), the variance of the electron beam energy distribution is

$$\sigma_{\text{Comp}}^2 = \frac{E_e}{4\langle E_\gamma\rangle}\int_0^{E_\gamma^{\max}}\frac{1}{\sigma_c}E_\gamma^2\frac{d\sigma_c}{dE_\gamma}dE_\gamma = \frac{E_e}{4\langle E_\gamma\rangle}\sigma_{E_\gamma}^2, \tag{23}$$

where $\sigma_{E_\gamma}^2$ is a variance of the scattered photon energy spectrum. On the other hand, the variance of the electron transverse angular deflection is given by

$$\langle\theta_e^2\rangle = \frac{E_e}{2\langle E_\gamma\rangle}\int_0^{E_\gamma(\theta_e^{\max})}\frac{1}{\sigma_c}\theta_e^2(E_\gamma)\frac{d\sigma_c}{dE_\gamma}dE_\gamma = \frac{E_e}{2\langle E_\gamma\rangle}\sigma_{\theta_e}^2\Big|_{E_\gamma}, \tag{24}$$

where $\sigma_{\theta_e}^2\big|_{E_\gamma}$ is a variance of the scattered electron angular distribution integrated over the scattered photon energy spectrum.

From the two expressions above, it becomes clear that the calculation of the equilibrium energy spread and transverse emittance involves the knowledge of the differential cross section of the Compton scattering. This allows us, according to Eqs. (23) and (24) to extend the Campbell's theorem method to the case of the polarized Compton scattering.

IV. ANALYTICAL SOLUTION IN A LOW RECOIL APPROXIMATION

Analytical expressions can be found for the general case of "head-on" collisions, unpolarized relativistic beams and assuming a negligible recoil, so that $x \ll 1$ which implies $E_e - E_\gamma \approx E_e$. This is a practical example providing the closed-form expressions for the equilibrium emittance and energy spread.

Considering Eq. (2) with $r = \frac{y}{x(1-y)}$ the Compton differential cross section is

$$\frac{d\sigma_c}{dy} = \frac{2\pi r_e^2}{x}\left(1 + \frac{1}{1-y} - y - \frac{4y\left(1 - \frac{y}{x(1-y)}\right)}{x(1-y)}\right.$$
$$\left. + P_eP_c\frac{(2-y)\left(1 - \frac{2y}{x(1-y)}\right)y}{1-y}\right) \tag{25}$$

and substituting $y = \frac{E_\gamma}{E_e}$ and $x = \frac{4\gamma^2E_L}{E_e}$ it reads:

$$\frac{d\sigma_c}{dE_\gamma} = \frac{\pi r_e^2}{2\gamma^2E_L}\left(\frac{E_e - E_\gamma}{E_e} + \frac{E_e}{E_e - E_\gamma}\right.$$
$$- \frac{E_eE_\gamma\left(1 - \frac{E_eE_\gamma}{4\gamma^2E_L(E_e-E_\gamma)}\right)}{\gamma^2E_L(E_e - E_\gamma)}$$
$$\left. + P_eP_c\frac{E_\gamma\left(2 - \frac{E_\gamma}{E_e}\right)\left(1 - \frac{E_eE_\gamma}{2\gamma^2E_L(E_e-E_\gamma)}\right)}{E_e - E_\gamma}\right), \tag{26}$$

where it is still possible to separate the unpolarized and the polarized contributions. Taking into account only the unpolarized part and imposing $E_e - E_\gamma \approx E_e$ one obtains the following expression for the differential cross section:

$$\frac{d\sigma_c^{np}}{dE_\gamma} = \frac{\pi r_e^2}{2\gamma^2E_L}\left(2 - \frac{E_\gamma\left(1 - \frac{E_\gamma}{4\gamma^2E_L}\right)}{\gamma^2E_L}\right) \tag{27}$$

and rearranging the terms the final expression reads:

$$\frac{d\sigma_c^{np}}{dE_\gamma} = \frac{\pi r_e^2(E_\gamma^2 - 4\gamma^2E_\gamma E_L + 8\gamma^4E_L^2)}{8\gamma^6E_L^3}. \tag{28}$$

In these approximations the integration of Eq. (28) gives the total cross section which is equal in this case to the Thomson cross section σ_T:

$$\int_0^{4\gamma^2E_L}\frac{d\sigma_c^{np}}{dE_\gamma}dE_\gamma = \sigma_T = \frac{8}{3}\pi r_e^2. \tag{29}$$

At this point, plugging the differential cross section [Eq. (28)] in the integrals of Eqs. (18) and (23), it is possible to provide the analytical form for the average and the variance of the emitted photon energy:

$$\langle E_\gamma\rangle = 2E_L\gamma^2 \quad \text{and} \quad \sigma_{E_\gamma}^2 = \frac{28}{5}E_L^2\gamma^4. \tag{30}$$

Inserting the above relations into Eq. (23), the relative equilibrium energy spread reads:

$$\delta_E^{\text{Comp}} \equiv \frac{\sigma_{\text{Comp}}}{E_e} = \sqrt{\frac{7}{10}\frac{E_L\gamma}{m_ec^2}} = \sqrt{\frac{7}{10}\frac{\lambda_C}{\lambda_L}}\gamma, \tag{31}$$

where $\lambda_C = h/m_ec \approx 2.43 \times 10^{-12}$ m is the Compton wavelength of the electron and λ_L is the wavelength of the laser. It can be pointed out that the energy spread induced by the Compton scattering is independent of the laser power and machine parameters.

In order to evaluate also the emittance, the Compton differential cross section and the average energy have to be plugged into Eq. (24), where the integration is done over the whole electron angular range after the Compton

scattering. Given the approximations discussed above, the energy of the scattered photon E_γ corresponding to the maximum electron deflection θ_e^{max} [see Eq. (22)] is found to be $E_\gamma(\theta_e^{max}) = 2\gamma^2 E_L$. Evaluating the integral in Eq. (24), one gets $\sigma_{\theta_e}^2|_{E_\gamma} = \frac{6E_L^2\gamma^2}{5E_e^2}$. Therefore, the variance of the electron transverse angular deflection can be written as:

$$\langle\theta_e^2\rangle = \frac{3}{10}\frac{E_L}{\gamma m_e c^2} = \frac{3}{10}\frac{\lambda_C}{\lambda_L}\frac{1}{\gamma}. \qquad (32)$$

Projecting it onto the x-y plane, one has $\langle\theta_{x,y}^2\rangle = \frac{1}{2}\langle\theta_e^2\rangle$.

As stated before, the transverse emittance is related to the angular spread of the electron beam σ_{θ_e} as

$$\epsilon_{x,y}^{Comp} \equiv \epsilon_\perp^{Comp} = 2\langle\theta_{x,y}^2\rangle\beta^* = \frac{3}{10}\frac{\lambda_C}{\lambda_L}\frac{1}{\gamma}\beta^*, \qquad (33)$$

that corresponds to the equilibrium normalized emittance of

$$\epsilon_{n\perp}^{Comp} = \gamma\epsilon_\perp^{Comp} = \frac{3}{10}\frac{\lambda_C}{\lambda_L}\beta^*. \qquad (34)$$

Assuming a Compton ring working at 1.3 GeV electron beam energy with the IP beta function $\beta^* = 1$ cm and together with a 1 μm (1.17 eV) wavelength laser, the normalized emittance due to the Compton scattering is $\sim 7 \times 10^{-9}$ m $\cdot$ rad. The equilibrium energy spread according to Eq. (31) is $\sim 6\%$.

Using different methods, the corresponding results obtained in [40,41] are in full agreement with the Campbell's theorem method. Only in [25], there is a difference given by a factor $1/\sqrt{2}$ in the calculated equilibrium energy spread. However, in a later publication [42] the author pointed out this difference and gave the proper result.

In the case of a "nonzero" collision angle ϕ (see Fig. 1) between the laser pulse and the electron beam ($\phi = \pi$ signifies the "head-on" collisions) in the formulas for the equilibrium energy spread [Eq. (31)] and the normalized transverse emittance [Eq. (34)], the wavelength of the laser λ_L should be substituted by the $\frac{2\lambda_L}{1-\cos\phi}$ in order to extend the considerations for the case of oblique collisions [41,43].

V. NUMERICAL SOLUTION FOR POLARIZED INITIAL STATES

Often it is not possible to get an analytical solution, but numerical integration can easily provide the correct estimations. As an application example the Compton scattering including the polarization of the initial states has been considered. In this case Eq. (25) has been taken into account and the expressions Eqs. (23) and (24) have been integrated numerically.

Since the asymmetry in the Compton differential cross section between the $P_c P_e = \pm 1$ states is small at moderate electron beam energy ($E_e < $ few GeV) and becomes very large at higher electron energies, an example considering a 10 GeV electron beam energy and a 1 μm wavelength laser has been taken into account. In this case, changing the initial polarization states introduces $\sim 18\%$ of variation in the normalized transverse equilibrium emittance (see Fig. 2). On the other hand, for the relative energy spread, as illustrated in Fig. 2a, this results in a $\sim 2\%$ deviation. The emittance and energy spread dependence on the polarization product $P_c P_e$ is almost linear at low electron beam energy ($E_e \sim 1$ GeV), although at energies higher than a few tens of GeV it shows rather nonlinear behavior. It is worth pointing out that varying the initial polarization states, there is not a simultaneous net cooling effect in either emittance or energy spread in respect to the unpolarized case $P_c P_e = 0$.

Given that the polarized cross section asymmetry is strongly dependent on the energy, the relative variation of the energy spread and of the emittance have been evaluated in the $P_c P_e = \pm 1$ range for different beam energies (see Figs. 3b and 3a). Strong variations are expected for the
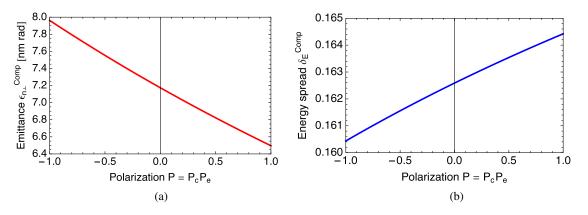

FIG. 2. Compton dynamics including the polarization of the initial states. (a) and (b) show, respectively, the equilibrium normalized transverse emittance and relative energy spread as a function of the product of electron and laser photon polarizations for a 10 GeV electron beam energy. A 1 μm wavelength laser and an IP beta function $\beta^* = 1$ cm are taken into account.
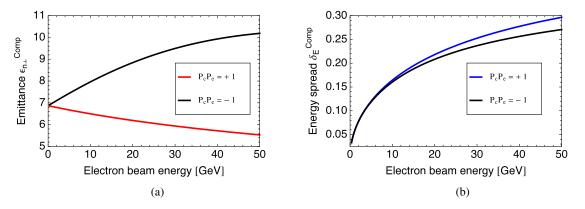
FIG. 3.   Compton dynamics including the polarization of the initial states. (a) and (b) show, respectively, the deviations in the equilibrium normalized transverse emittance and relative energy spread (see Fig. 2) at different electron beam energies varying the polarization product in the $P_c P_e = \pm 1$ range. The collision parameters are the same as for Fig. 2.

high energy beams. This has to be taken into account in Compton polarimetry and beam energy measurements by evaluating the total equilibrium energy spread or emittance including the synchrotron radiation emission. This is the subject of the next paragraph.

VI. EQUILIBRIUM ENERGY SPREAD AND EMITTANCE IN A COMPTON RING

In a Compton storage ring configuration the final equilibrium energy spread is the result of both the Compton and the synchrotron emission processes. In this case, supposing that synchrotron radiation and Compton scattering are uncorrelated, the final energy variance will be the sum of the weighted variances of the two different processes:

$$\sigma_E^2 = \frac{\sigma_{\text{Synch}}^2 (\Delta E)_{\text{Synch}} + \sigma_{\text{Comp}}^2 (\Delta E)_{\text{Comp}}}{(\Delta E)_{\text{Synch}} + (\Delta E)_{\text{Comp}}}, \qquad (35)$$

where σ_{Synch}, σ_{Comp} are, respectively, the equilibrium energy spread in presence of the synchrotron radiation and Compton scattering; $(\Delta E)_{\text{Synch}}$, $(\Delta E)_{\text{Comp}}$ are the energy losses per turn and per particle caused by synchrotron radiation and Compton scattering.

The natural energy spread and energy loss due to emission of the synchrotron radiation is determined by the energy of the stored electron beam and the lattice design (by the bending radii of the dipoles in the case of an isomagnetic ring) [44].

$$\delta_E^{\text{Synch}} \equiv \frac{\sigma_{\text{Synch}}}{E_e} = \sqrt{\frac{C_q \gamma^2 I_{s3}}{(2I_{s2} + I_{s4})}} = \sqrt{\frac{C_q \gamma^2 I_{s3}}{J_e I_{s2}}}, \qquad (36)$$

$$(\Delta E)_{\text{Synch}} = \frac{C_\gamma}{2\pi} E_e^4 I_{s2}, \qquad (37)$$

where I_{s2} and I_{s3} are the synchrotron radiation integrals, $C_\gamma = 8.846 \times 10^{-5} \text{ m/GeV}^3$ and $C_q = 3.8319 \times 10^{-13} \text{ m}$

are the quantum coefficients and J_e is the damping partition number of the longitudinal plane.

The energy spread induced by Compton scattering is given by Eq. (31) and the energy loss per turn and per particle is set to the average energy of the emitted photons defined by Eq. (18), that is $(\Delta E)_{\text{Comp}} = \mathcal{F} \langle E_\gamma \rangle = \mathcal{L} \sigma_c \langle E_\gamma \rangle$.

To provide a numerical estimation we can give a basic example taking into account an isomagnetic ring with $\rho = 5.37 \text{ m}$ (bending radius of the ATF ring in KEK, Japan) and the Compton "head-on" collisions with $x \ll 1$ and round beams. In this case Eqs. (36) and (37) can be expressed as:

$$\delta_E^{\text{Synch}}|_{\text{iso}} = \sqrt{\frac{C_q \gamma^2}{J_e \rho}}, \qquad (38)$$

$$(\Delta E)_{\text{Synch}}|_{\text{iso}} = \frac{C_\gamma}{\rho} E_e^4, \qquad (39)$$

and the luminosity of the Compton collisions reads:

$$\mathcal{L} = N_e N_{ph} \frac{1}{2\pi} \frac{1}{2\sigma_{e,L}^2}, \qquad (40)$$

where $\sigma_{e,L}$ is the electron or the laser RMS beam size in the IP. As a reference normalization for the Compton interaction probability we set the laser pulse energy in a way that we have a unit probability to have one scattering per turn per particle with the laser and electron beam sizes of 25 μm:

$$\mathcal{L}\sigma_c = \sigma_c N_e N_{ph} \frac{1}{2\pi} \frac{1}{2\sigma_{e,L}^2} = 1. \qquad (41)$$

Solving Eq. (41), one gets the laser pulse energy equals to 22 J. Substituting and integrating Eq. (35) it is possible to evaluate the partial impact of the Compton backscattering and synchrotron radiation on the beam dynamics as a
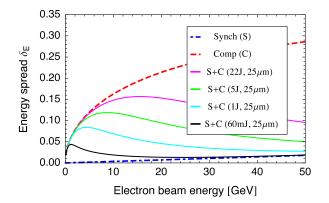
FIG. 4. Compton ring relative energy spread. The natural energy spread ("Synch") is calculated for an isomagnetic ring with magnetic radius of 5.37 m. A 1 μm wavelength laser is used for estimating the Compton induced energy spread ("Comp"). The final equilibrium energy spread ("S + C") is given for four different laser pulse energies and for the electron and laser beam size of $\sigma_{e,L} = 25$ μm.
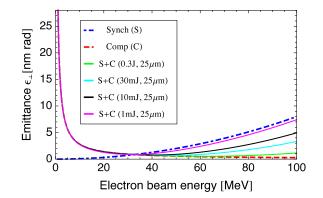

FIG. 5. ThomX ring equilibrium transverse emittance. The natural emittance ("Synch") is calculated taking into account the lattice of the ThomX ring. A 1 μm wavelength laser is used for estimating the Compton induced emittance ("Comp"). The final equilibrium transverse emittance ("S + C") is given for four different laser pulse energies and for the electron and laser beam size of $\sigma_{e,L} = 25$ μm.

function of the electron beam energy and for different laser pulse energies (see Fig. 4). At high energy the synchrotron damping dominates and the asymptotic behavior follows the synchrotron dynamics characteristics, especially for the low Compton flux. On the other hand, the Compton effect is very effective at low energy, where a net energy spread increase is appearing. The derivative change as a function of the beam energy is noticeably a function of the laser pulse energy. A numerical analysis of the derivative change location for different laser pulse energies shows that the normalized electron beam energy at which the final equilibrium energy spread reaches its maximum is related to the normalized electron beam energy at which the energy losses given by the two mechanisms are equal, i.e.,

$$\frac{E_e^i(\delta_E^{\max})}{E_e^0(\delta_E^{\max})} = \frac{E_e^i((\Delta E)_{\text{Comp}} = (\Delta E)_{\text{Synch}})}{E_e^0((\Delta E)_{\text{Comp}} = (\Delta E)_{\text{Synch}})}, \quad (42)$$

where the superscript i indicates the values taken at different laser pulse energies and E_e^0 is a reference energy for normalization.

It is worth pointing out that as opposed to the case of the equilibrium defined only by the Compton scattering, the result obtained considering the Compton scattering and synchrotron radiation is a function of the Compton collision luminosity.

The same analysis worked out for the energy spread can be done in the case of the transverse emittance. In this case we have that:

$$\epsilon_\perp = \frac{\epsilon_{\text{Synch}}(\Delta E)_{\text{Synch}} + \epsilon_{\text{Comp}}(\Delta E)_{\text{Comp}}}{(\Delta E)_{\text{Synch}} + (\Delta E)_{\text{Comp}}}. \quad (43)$$

Taking the expression for the natural beam emittance [44] and assuming the previous Compton collision parameters, one can evaluate the relative contributions in the case

of the ThomX ring [4] (bending radius $\rho = 0.35$ m) as illustrated in Fig. 5. It is possible to appreciate the net transverse cooling effect of the Compton scattering in a large energy range. For lower energies, the contribution provided by the Compton scattering is larger and the resulting emittance defined by Eq. (43) follows the Compton induced emittance (see Fig. 5 where all four curves "S + C" coincide with the curve calculated for the Compton induced emittance). At higher energy, the synchrotron damping again dominates and the asymptotic behavior follows the emittance given by the synchrotron dynamics.

In a real Compton ring the energy spread and emittance are also affected by different collective effects leading to the increase of the 6D-emittance as a function of the electron bunch charge. By applying the Campbell's theorem and the weighted average sum it should be possible to extend this analysis to a more complex scenario, like including the coherent synchrotron radiation (CSR) effects.

VII. CONCLUSIONS

In the framework of the Compton ring dynamics the laser photon-electron scattering can be seen as a shot noise process. In this context, it is possible to evaluate the equilibrium energy spread and emittance of the beam by means of Campbell's theorem. This method allows us to extend the calculations to the numerical evaluation of polarized beam equilibrium as well. An example at 10 GeV was provided together with the relative variation of the equilibrium energy spread and emittance as a function of energy showing a few percent variation for the energy spread but a bigger contribution for the emittance. The relative contributions as a function of energy for two different polarization states have been illustrated showing a slow increase. The final analytical

results given in the low recoil approximation are in perfect agreement with those obtained by matching the laser cooling and quantum excitation terms in the Compton backscattering. They show that the equilibrium emittance and energy spread are not dependent on the luminosity but depend only on the differential cross section. An extrapolation to the case of the equilibrium emittance and energy spread given by both Compton and synchrotron radiation has been illustrated. This shows that in this case, the equilibrium state is a function of the Compton collision luminosity. These methods can be extended to other radiation mechanisms and instability processes.

[1] G. A. Krafft and G. Priebe, Rev. Accel. Sci. Techol. **03**, 147 (2010).

[2] J. Bonis et al., JINST **7**, P01017 (2012).

[3] C. Vaccarezza, O. Adriani et al., in Proceedings of the 3rd International Particle Accelerator Conference, New Orleans, LA, 2012 (IEEE, Piscataway, NJ, 2012), p. 1086.

[4] C. Bruni, R. Chiche et al., Report No. LAL RT 09/28; Report No. SOLEIL/SOU-RA-2678, 2009.

[5] R. Ruth, "First science from the compact light source: A miniature synchrotron for your home lab," http://eurekalert.org/pub_releases/2009-01/lti-fsf010609.php.

[6] ELI Nuclear Physics working groups, "The white book of ELI Nuclear Physics," Reference available at http://www.eli-np.ro/documents/ELI-NP-WhiteBook.pdf.

[7] C. Barty and F. Hartemann, Lawrence Livermore Laboratory Report No. UCRL-TR-206825, 2004.

[8] R. Hajima, T. Hayakawa, N. Kikuzawa, and E. Minehara, J. Nucl. Sci. Technol. **45**, 441 (2008).

[9] W. Graves, W. Brown, F. Kaertner, and D. Moncton, Nucl. Instrum. Methods Phys. Res., Sect. A **608**, S103 (2009).

[10] G. Priebe, D. Filippetto, O. Williams et al., Nucl. Instrum. Methods Phys. Res., Sect. A **608**, S109 (2009).

[11] T. Yamazaki, T. Noguchi, S. Sugiyama, T. Mikado, M. Chiwaki, and T. Tomimasu, IEEE Trans. Nucl. Sci. **32**, 3406 (1985).

[12] H. Ohgaki, H. Toyokawa, K. Kudo, N. Takeda, and T. Yamazaki, Nucl. Instrum. Methods Phys. Res., Sect. A **455**, 54 (2000).

[13] F. Glotin, J.-M. Ortega, R. Prazeres, G. Devanz, and O. Marcouillé, Phys. Rev. Lett. **77**, 3130 (1996).

[14] L. Federici, G. Giordano, G. Matone et al., Nuovo Cimento Soc. Ital. Fis. **59B**, 247 (1980).

[15] V. G. Nedorezov, A. A. Turinge, and Yu. M. Shatunov, Phys. Usp. **47**, 341 (2004).

[16] D. Nutarelli, M. E. Couprie, L. Nahon, R. Bakker, A. Delboulbe, R. Roux, B. Visentin, and M. Billardon, Nucl. Instrum. Methods Phys. Res., Sect. A **407**, 459 (1998).

[17] V. N. Litvinenko et al., Phys. Rev. Lett. **78**, 4569 (1997).

[18] T. Russew, Ph.D. thesis, Grenoble University, 1995.

[19] H. Ohgaki, T. Noguchi, S. Sugiyama, T. Yamazaki, T. Mikado, M. Chiwaki, K. Yamada, R. Suzuki, and N. Sei, Nucl. Instrum. Methods Phys. Res., Sect. A **353**, 384 (1994).

[20] M. Hosaka, H. Hama, K. Kimura, J. Yamazaki, and T. Kinoshita, Nucl. Instrum. Methods Phys. Res., Sect. A **393**, 525 (1997).

[21] H. R. Weller, M. W. Ahmed, H. Gao, W. Tornow, Y. K. Wu, M. Gai, and R. Miskimen, Prog. Part. Nucl. Phys. **62**, 257 (2009).

[22] "The compact light source," http://www.lynceantech.com/.

[23] A. Zelinsky, " Status of Kharkov X-ray generator based on Compton scattering NESTOR," Stanford Linear Accelerator Center (SLAC), 2005.

[24] V. Telnov, Phys. Rev. Lett. **78**, 4757 (1997).

[25] Z. Huang and R. D. Ruth, Phys. Rev. Lett. **80**, 976 (1998).

[26] E. Bulyak, P. Gladkikh, V. Skomorokhov, T. Omori, J. Urakawa, K. Moenig, and F. Zimmermann, Phys. Rev. ST Accel. Beams **9**, 094001 (2006).

[27] V. Strakhovenko, X. Artru, R. Chehab, and M. Chevallier, Nucl. Instrum. Methods Phys. Res., Sect. A **547**, 320 (2005).

[28] I. F. Ginzburg, G. L. Kotkin, V. G. Serbo, and V. I. Telnov, Nucl. Instrum. Methods Phys. Res. **205**, 47 (1983).

[29] I. F. Ginzburg, G. L. Kotkin, S. L. Panfil, V. G. Serbo, and V. I. Telnov, Nucl. Instrum. Methods Phys. Res., Sect. A **219**, 5 (1984).

[30] D. Y. Ivanov, G. Kotkin, and V. Serbo, Eur. Phys. J. C **36**, 127 (2004).

[31] N. Campbell, Proc. Cambridge Philos. Soc. **15**, 310 (1909).

[32] J. F. C. Kingman, Poisson Processes (Oxford University Press, New York, 1993), Vol. 3.

[33] A. Papoulis, Probability, Random Variables, and Stochastic Processes (McGraw-Hill, New York, 1991), 3rd ed.

[34] N. Wax, Selected Papers on Noise and Stochastic Processes (Dover, New York, 2003).

[35] M. Sands, Stanford Linear Accelerator Center Report No. SLAC-R-121, 1970.

[36] A. Hofmann, The Physics of Synchrotron Radiation (Cambridge University Press, Cambridge, England, 2004), Vol. 20.

[37] A. Hofmann, in CAS-CERN Accelerator School: Proceedings of the 5th Advanced Accelerator Physics Course, edited by S. Turner (CERN, Geneva, Switzerland, 1995), pp. 259–274.

[38] H. Wiedemann, Particle Accelerator Physics I: Basic Principles and Linear Beam Dynamics (Springer Verlag, Berlin, 1999), Vol. 1.

[39] V. Telnov, Nucl. Instrum. Methods Phys. Res., Sect. A **355**, 3 (1995).

[40] V. Telnov, Nucl. Instrum. Methods Phys. Res., Sect. A **455**, 80 (2000).

[41] J. Urakawa, K. Kubo, N. Terunuma et al., Nucl. Instrum. Methods Phys. Res., Sect. A **532**, 388 (2004).

[42] Z. Huang, in The Physics of High Brightness Beams. Proceedings of the 2nd ICFA Advanced Accelerator Workshop, edited by J. Rosenzweig and L. Serafini (World Scientific, Singapore, 1999).

[43] J. Urakawa and F. Zimmermann, "Considerations on laser cooling at the ATF damping ring (old draft)," (unpublished).

[44] A. Chao, Handbook of Accelerator Physics and Engineering (World Scientific, Singapore, 1999).